

The effects of high temperature on the high-pressure behavior of CeO₂

This article has been downloaded from IOPscience. Please scroll down to see the full text article.

2007 J. Phys.: Condens. Matter 19 425213

(<http://iopscience.iop.org/0953-8984/19/42/425213>)

View [the table of contents for this issue](#), or go to the [journal homepage](#) for more

Download details:

IP Address: 129.252.86.83

The article was downloaded on 29/05/2010 at 06:13

Please note that [terms and conditions apply](#).

The effects of high temperature on the high-pressure behavior of CeO₂

Wansheng Xiao¹, Dayong Tan¹, Yanchun Li² and Jing Liu²

¹ Guangzhou Institute of Geochemistry, Chinese Academy of Sciences, Guangzhou 510640, People's Republic of China

² High Energy Physics Institute, Chinese Academy of Sciences, Beijing 100049, People's Republic of China

E-mail: wsxiao@gig.ac.cn

Received 3 August 2007

Published 18 September 2007

Online at stacks.iop.org/JPhysCM/19/425213

Abstract

Raman spectrum and angle-dispersive x-ray diffraction (ADXRD) measurements have been performed to investigate the effects of high temperature on the high-pressure behavior of bulk CeO₂. A phase transformation of CeO₂ from fluorite to PbCl₂-type structure occurs at 12.0 GPa and is completed at 14.2 GPa after the sample is heated, and the phase transition pressure decreases by nearly 20 GPa compared with that at room temperature. On decompression, the high-pressure phase of CeO₂ remains down to 2.2 GPa, and it changes back to a cubic structure at ambient conditions. At a pressure of 22.1 GPa, a 6.4% lattice volume difference between the fluorite and PbCl₂-type structures was observed. The lattice volume of fluorite phase obtained in the areas that have been heated is about 1% less than that obtained in the areas that have not been heated. Besides prompting the phase transition of CeO₂, high temperature also anneals the sample and leads a small reduction in lattice volume of the fluorite phase. The zero-pressure bulk modulus of the fluorite phase of CeO₂ after annealing is calculated to be about 200 GPa with an assumed pressure derivative of four, which is smaller than that of former x-ray diffraction experiments at room temperature.

1. Introduction

CeO₂ is one of the extensively studied dioxides because of its technological applications and theoretical implications [1–6]. The pressure-induced phase transition of CeO₂ has been the subject of some recent studies [7–12] because it can be related to the systematics of the high-pressure behavior of the fluorite-type compounds [13–19]. The bulk modulus of CeO₂ obtained by high-pressure experiments was also used to test the theoretical calculation methods [15, 20, 21]. The Raman spectra from bulk CeO₂ up to 35 GPa demonstrate that the cubic structure of CeO₂ transforms to an orthorhombic PbCl₂-type phase (*Pnam*) at 31 GPa,

and recovers its initial phase at 11 GPa during decompression [7]. The high-pressure x-ray diffraction experiments also reported a phase transition from fluorite to an orthorhombic PbCl_2 structure at around 31.5 GPa, in excellent agreement with the Raman result [8, 9]. The phase transition from fluorite to PbCl_2 -type structure results in a volume collapse of 7.5–9.8% [8, 9]. High-pressure studies of nanosized CeO_2 at room temperature show that the cubic structure changes to a PbCl_2 -type structure at pressures of 22.3–26.5 GPa, which are much lower than that for bulk material [10, 11], and the high-pressure phase remains under pressures down to 1.8 GPa during decompression [11].

Based on *in situ* x-ray diffraction results at room temperature, Duclos *et al* [8] reported that the phase transformation of CeO_2 from fluorite to an orthorhombic PbCl_2 -type structure began at about 31 GPa and was completed at about 38 GPa. The Raman results [7] also show a 20 GPa hysteresis of the high-pressure phase upon pressure reversal. Those phenomena indicate that this transition is kinetically hindered or sluggish. The pressure-induced phase transition from fluorite to an orthorhombic PbCl_2 -type structure is a first-order transition, and the diffusion of metal atoms and reconstruction of bonds are also involved in the transition process. The transition can be visualized as the result of cations in the (111) planes of fluorite structure moving along the [111] axis into adjacent anions planes, which lowers the symmetry and increases the cation coordination from 8 to 9 to form the orthorhombic PbCl_2 -type structure [22]. The atom diffusion coefficient can be expressed as follows:

$$D = D_0 e^{-\Delta G/RT} \quad (1)$$

where D is the diffusion coefficient, D_0 is a constant, and ΔG is activation energy of migration. The term ΔG is the function of the environments around the migrating atoms, such as crystal structure, chemical bond, pressure, and so on. The factor of temperature (T) in formula (1) is an individual variable which reflects its important effect on atomic migration. The fluorite-related lanthanide oxides show unusual diffusion properties. Until about 1200 °C is achieved, the metal atomic mobility of rare earth elements in a solid does not become significant [23]. This means that a large ΔG exists. From kinetic considerations, a high temperature (up to 1200 °C) should improve the mobility of atoms to reach a thermodynamic equilibrium state and lower the pressure for the phase transition of CeO_2 . Up to now, most high-pressure experiments on CeO_2 , both bulk and nanosized materials, have been conducted at room temperature [7–11, 15]. A laser-heating experiment on CeO_2 at 25–28 GPa and around 1000 °C resulted in the appearance of two new very weak diffraction lines at 2.966 and 2.804 Å when it was quenched to ambient condition [24]. Here we present the experimental results on the effects of high temperature on the high-pressure behavior of bulk CeO_2 .

2. Experimental details

A powder sample of CeO_2 (reagent grade, purity > 99.9%) was heated at a temperature of 1200 °C for 2 h, and then was cooled to room temperature in the furnace. A Mao–Bell-type diamond anvil cell (DAC) was employed to generate high pressure; the diameter of the anvil culet was 400 μm . T301 stainless steel with thickness of 0.25 mm was used as a gasket, which was preindented to about 40 μm . The sample of CeO_2 was packed into the sample hole of 110 μm diameter with two fine ruby chips for pressure determination using the calibration of Mao *et al* [25]. A YAG laser beam of 1.064 μm wavelength was focused to about a few microns by a 20 \times object lens, and the sample was heated locally in a one-sided laser beam scanning mode. We cannot measure the heating temperature via the black-body emission technique or simply by an infrared (IR) thermometer due to lack of corresponding apparatus in our YAG laser heating system, so the heating temperature was estimated by the brightness of the heated spot

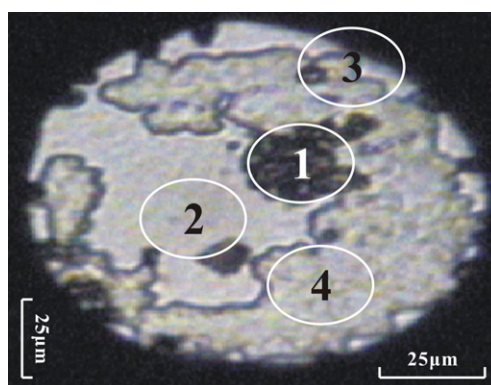


Figure 1. A micrograph of the sample at 22.1 GPa and the locations of x-ray diffraction patterns. (This figure is in colour only in the electronic version)

observed by the eyes through a microscope, which induces considerable error. Considering that the aim of using a YAG laser to heat the sample in our experiment is to eliminate the hysteresis of the phase transition, this considerable error in the temperature would not change the conclusions of this paper. Nevertheless, the considerable temperature uncertainty would make it hard to discuss some questions. The sample was heated at pressures of 12.0, 14.2 and 22.1 GPa, respectively. In the process of heating, about half of the sample was heated moderately and the temperature was estimated to be about 1000 °C; and an area of about 25 μm in diameter was heated intensively and the temperature was estimated to be more than 1200 °C, at which it became dark as shown in figure 1.

Both the Raman and x-ray diffraction measurements in this study were recorded at room temperature. The Raman spectra were excited with 514.5 nm radiation from an argon ion laser and recorded by a Renishaw 2000 Raman spectrometer in the backscattered geometry. A 30 \times objective with 16 mm working distance was used to focus the excited laser beam and collect the Raman scattering. A single 1800 g mm^{-1} grating was used to disperse the Raman scattering which was then recorded by a CCD detector at a resolution of 2 cm^{-1} . It should be noted that the notch filter in the Renishaw 2000 Raman spectrometer starts to eliminate the Rayleigh lines at about 150 cm^{-1} . This makes the determination of bands below 200 cm^{-1} difficult and without reliability.

An angle-dispersive powder x-ray diffraction (ADX) experiment on CeO_2 at a pressure of 22.1 GPa has been carried out at room temperature on the bending magnet beam line BL-18C of the Photon Factory in the High Energy Accelerator Research Organization (KEK). The x-ray was monochromatized to a wavelength of 0.61651 Å with two Si(111) crystals, and focused in horizontal and vertical directions with two curved mirrors. A pinhole collimator placed in front of the DAC was used to limit the final beam size to 25 μm in diameter. The diffracted x-ray was detected with an imaging plate placed at a distance of about 238.89 mm which was calibrated by a standard sample of Ag. Five x-ray diffraction patterns were obtained at different areas in the sample chamber.

3. Results and discussion

3.1. Raman scattering

Raman spectra of CeO_2 at a few representative pressures are shown in figure 2 and table 1. At ambient conditions, CeO_2 exists in the fluorite structure, and a single strong first-order

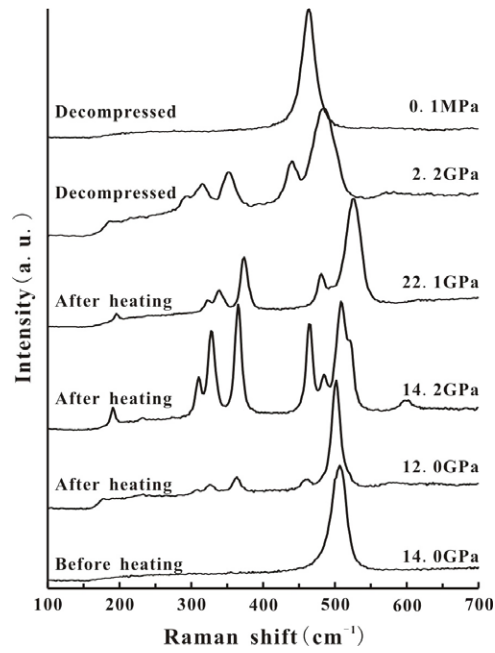


Figure 2. Representative Raman spectra of CeO₂ at different pressures.

Table 1. Raman frequencies of the PbCl₂-type structure of CeO₂ at different pressures¹.

Wavenumbers (cm ⁻¹)					
This study				Kourouklis <i>et al</i> [7]	
12.0 GPa	14.2 GPa	22.1 GPa	2.2 GPa	22.6 GPa	13.4 GPa
	599w	617			
501	520s	526	484	535	507
	509s				
	485w	494			
460	465s	481	439	488	460
363	365s	374	352	374	365
		345w			
326	328s	339	315	355	327
308	311m	323	293	334	310
231	232w	241			
	191m	196		200	192
				141	132

¹ w = weak, m = medium, s = strong.

Raman band at 464 cm⁻¹ is assigned to the three degenerate vibrations of the T_{2g} mode of this structure [26]. The T_{2g} Raman band shifts to 506 cm⁻¹ at a pressure of 14 GPa, showing a shift ratio of about 3.0 cm⁻¹ GPa⁻¹, and no phase transition occurs, which is consistent with the results of [7]. After being heated by the YAG laser beam and with a pressure change to 12.0 GPa, five new Raman peaks appear besides the strongest peak at 501 cm⁻¹. This means that a phase transition of CeO₂ occurs at this pressure after heating, and the 501 cm⁻¹ peak possibly belongs to the mixed bands of the T_{2g} band of the fluorite structure and some bands of the new high-pressure phase, according to the following results. The Raman spectrum of the sample after it had been heated intensively at a pressure of 14.2 GPa, shown in figure 2

and table 1, presents ten distinct Raman active bands between 150 and 700 cm^{-1} with good quality, and the intense T_{2g} band of the fluorite structure is replaced by at least four bands, which confirms that the CeO_2 with fluorite structure changes to a new high-pressure phase completely. The sample was subjected to a pressure of 22.1 GPa and heated again; the Raman spectrum is identical to that at 14.2 GPa except that all bands shift to higher frequencies with different pressure dependences and the relative intensity between bands changes somewhat.

In comparison with the high-pressure Raman results from single-crystal CeO_2 at room temperature of Kourouklis *et al* [7], shown in table 1, the Raman spectra of CeO_2 after being treated under high temperature at different pressures in this study are similar to those of the high-pressure phase of CeO_2 , which was suggested to be a PbCl_2 -like structure with space group $Pnam$ by Kourouklis *et al* [7]. The subsequent x-ray diffraction results at room temperature indicate that the cubic structure of CeO_2 transforms to the PbCl_2 -type structure at about 31 GPa [8]. Thus, we consider that the high-pressure phase of CeO_2 , occurring at pressures as low as 12.0 GPa after the sample undergoes high-temperature treatment in this study, adopt the PbCl_2 -type structure. This conclusion was also confirmed by the x-ray diffraction result shown in the next section. Furthermore, the Raman spectra of the high-pressure phase of CeO_2 in this study include at least ten distinguishable bands in the range 150–700 cm^{-1} . In contrast, the Raman spectra of the high-pressure phase of CeO_2 , determined with a single crystal and employing argon or methanol–ethanol mixture in the ratio 4:1 as pressure media by Kourouklis *et al* [7], have seven bands in the range 100–600 cm^{-1} , with some broad bands that could be considered as possible overlapping modes. This means that the sample after being heated crystallizes better than at room temperature. Besides prompting a phase transition of CeO_2 and lowering the phase transition pressure remarkably (by as much as 20 GPa), the effects of high temperature also increase the metal atomic mobility to reach the thermodynamic equilibrium state.

According to group theory, the optical vibration modes of the PbCl_2 -type structure ($Pnam$) are expected to be 18 Raman-active bands [22]: $6A_g + 6B_{1g} + 3B_{2g} + 3B_{3g}$. We cannot assign the Raman bands based only on the results of this study due to the limitation of the determination method, and we cannot either find the assignment even for dioxides adopting the PbCl_2 -type structure in the literature. We consider the fact that the number of Raman bands for the high-pressure phase of the CeO_2 in this study is less than that expected for the PbCl_2 -type structure is because a limited range of wavenumber and overlapping bands may still exist. On decompression, the high-pressure phase of CeO_2 remains down to 2.2 GPa, and it changes back to the cubic structure at ambient conditions according to the Raman results. This result is different from that of [24].

3.2. X-ray diffraction

At a pressure of 22.1 GPa, five x-ray diffraction patterns were recorded from different areas in the sample chamber. The locations are illustrated in figure 1 (transmitted-light mode). The dark colored area was heated intensively, and diffraction patterns 1 and 5 were obtained from this area. The light colored area was moderately heated, and diffraction patterns 3 and 4 were obtained from this area. The transparent area was not heated, and diffraction pattern 2 was obtained from this area. The x-ray diffraction patterns are shown in figure 3. The x-ray diffraction patterns of 1 and 5, both as regards d -spacings and relative intensity, are identical with each other within errors, and the data for 3 and 4 are also the same except that in pattern 3 there appears a gasket peak from ϵ -iron (002).

Pattern 2 shows only five diffraction peaks, which can be indexed as (111), (200), (220), (311) and (222) of the cubic fluorite structure. This means that the sample of CeO_2 , which was

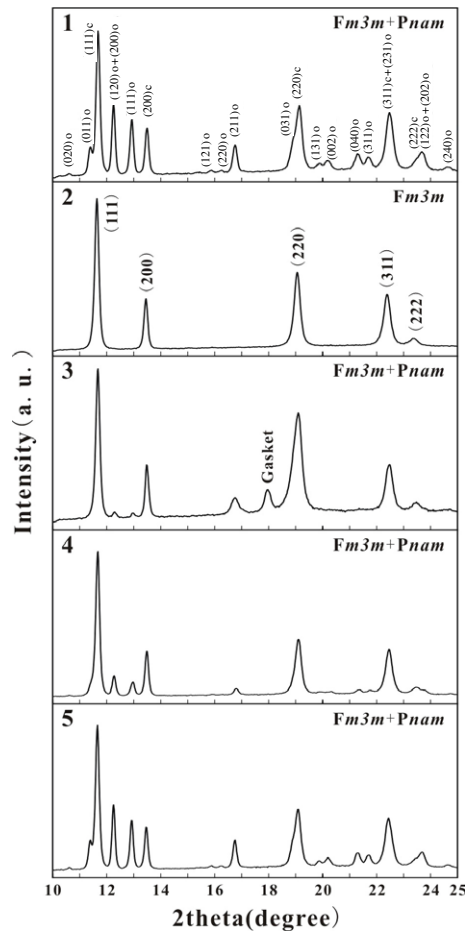


Figure 3. The x-ray diffraction patterns of CeO_2 at 22.1 GPa from different areas. Note that the $(hkl)_c$ represent the cubic peaks and $(hkl)_o$ represent orthorhombic peaks.

not heated, still keeps the fluorite structure at pressure of 22.1 GPa. In contrast, 20 diffraction peaks were observed in pattern 1. By comparing with pattern 2, we consider that 5 of the 20 peaks of pattern 1 belong to the cubic phase. The other 15 d -spacings can be indexed according to the orthorhombic PbCl_2 -type structure ($Pnam$). The results are shown in table 2. We suggest that pattern 1, which was collected from the area that had been heated intensively, reflects mixed phases of CeO_2 of fluorite and PbCl_2 -type structure. This phenomenon was possibly induced by the one-sided laser-heated method with a smaller heating spot and a small intensive heating area in the sample chamber. The temperature of the intensively heated side of the sample may be enough to induce a phase transformation of CeO_2 from fluorite to PbCl_2 -type structure. A large axial gradient of temperature exists due to the one-sided laser-heated method and smaller heating spot, so the temperature on the opposite side of the sample may not be enough to overcome the kinetic energy barrier to induce the phase transition, even though it should anneal the sample effectively.

According to the diffraction result of pattern 1, as shown in table 2, the phase transition from fluorite to PbCl_2 -type structure of CeO_2 induced a volume collapse of 6.4% at a pressure

Table 2. The ADXD results from CeO₂ at a pressure of 22.1 GPa.

<i>Pnam</i>			<i>Fm3m</i>										
1			1			2			3				
<i>hkl</i>	<i>d</i> _{obs} (Å)	<i>d</i> _{calc} (Å)	<i>hkl</i>	<i>d</i> _{obs} (Å)	<i>d</i> _{calc} (Å)	FWHM (deg)	<i>hkl</i>	<i>d</i> _{obs} (Å)	<i>d</i> _{calc} (Å)	FWHM (deg)	<i>hkl</i>	<i>d</i> _{obs} (Å)	<i>d</i> _{calc} (Å)
020	3.3351	3.3349	111	3.0294	3.0298	0.18	111	3.0408	3.0403	0.18	111	3.0309	3.0304
011	3.1059	3.1079	200	2.6238	2.6239	0.19	200	2.6317	2.6330	0.16	200	2.6237	2.6244
120	2.8879	2.8881	220	1.8546	1.8554		220	1.8620	1.8618	0.26	220	1.8566	1.8557
200	2.8879	2.8880	311	1.5833	1.5823		311	1.5878	1.5878	0.29	311	1.5824	1.5826
111	2.7373	2.7369	222	1.5157	1.5149		222	1.5212	1.5202	0.29	222	1.5146	1.5152
121	2.2328	2.2308		<i>a</i> = 5.2478(8) Å				<i>a</i> = 5.2660(9) Å				<i>a</i> = 5.2488(7) Å	
220	2.1823	2.1832		<i>V</i> = 144.52(7) Å ³				<i>V</i> = 146.03(8) Å ³				<i>V</i> = 144.61(6) Å ³	
211	2.1151	2.1156											
031	1.8776	1.8786											
131	1.7863	1.7865											
002	1.7575	1.7563											
040	1.6678	1.6675											
311	1.6372	1.6367											
231	1.5747	1.5747											
122	1.5015	1.5006											
202	1.5015	1.5006											
240	1.4446	1.4441											
				<i>a</i> = 5.7760(28) Å									
				<i>b</i> = 6.6699(15) Å									
				<i>c</i> = 3.5125(10) Å									
				<i>V</i> = 135.32(6) Å ³									

of 22.1 GPa. This value is smaller than the corresponding values of 7.5–9.8% obtained by Duclos *et al* [8] and Gerward and Olsen [9]. Comparing the lattice constants of the cubic phase of CeO₂ between patterns 1, 2 and 3, we find that pattern 1 and pattern 3 are identical with each other within error, but the volume of pattern 1 is smaller by about 1% than that of pattern 2. We do not think that this is induced by either experimental errors or pressure gradient in the sample chamber. The only difference between the two x-ray diffraction patterns is that they were collected from different areas in the same sample chamber, as shown in figure 1: one area was heated intensively, and the other one was not heated. We exclude the factor of pressure gradient based on the following evidence: (1) the pressures on the two ruby chips, which are located in area 1 and area 2 respectively, are 22.1 and 22.2 GPa, showing excellent agreement with each other. (2) The full width at half maximum (FWHM) of the diffraction peaks of the cubic structure of patterns 1 and 2, as shown in table 2, indicate that the hydrostaticity of the sample chamber is similar to that of adopting a methanol–ethanol mixture as the pressure medium [27]. Despite the fact that the sample was loaded without a pressure medium, the pressure gradient in the sample chamber was relaxed effectively by laser heating process. (3) Pattern 3 was collected at the edge of the sample chamber, from which there appears a gasket diffraction peak; the volume of its cubic structure was also about 1% smaller than that of pattern 2. (4) Employing the equation of state (EOS) parameters provided by Duclos *et al* [8] ($B_0 = 230$ GPa, $B'_0 = 4$) and Gerward *et al* [15] ($B_0 = 220$ GPa, $B'_0 = 4.4$), which were obtained at room temperature, and assuming the standard V_0 value of cubic CeO₂ to be 158.43 Å³ ($a_0 = 5.411$ Å), the pressure of the sample chamber is calculated to be 22.1 and 21.5 GPa respectively, according to the cubic phase volume of pattern 2 ($V = 146.03$ Å³), which shows excellent agreement with ruby scale. So we consider the pressure of the sample chamber to be 22.1 GPa, and the

volume difference of cubic phase between pattern 1 and pattern 2 is induced by the effect of high temperature. The mechanism remains unclear. We consider that the volume of fluorite phase of pattern 1 represents the thermodynamic equilibrium volume at a pressure of 22.1 GPa, and the volume of pattern 2 reflects the sluggish property of CeO₂ at high pressure. Due to the slow mobility of the Ce atom at room temperature, the volume of pattern 2 may indicate that the atoms of CeO₂ with fluorite structure could not adjust completely to their equilibrium positions, and may reflect that many defects exist in the structure, which lead to a relatively large volume.

The bulk modulus of the fluorite phase of bulk CeO₂ was deduced to be 220–236 GPa by fitting the Birch–Murnaghan equation of state based on x-ray diffraction experiments at room temperature [8, 9, 15]. By contrast with consistent experimental values, the theoretical results for the bulk modulus of CeO₂ show a large scatter [15, 20, 28, 29], and most of these are underestimated [15, 20, 28]. The bulk modulus of cubic CeO₂ cannot be obtained by fitting the Birch–Murnaghan equation of state based only on our x-ray diffraction results, since only one set of diffraction data at 22.1 GPa exists. However, we can calculate a bulk modulus B_0 of about 200 GPa by using the volume value ($V = 144.52 \text{ \AA}^3$, pattern 1) of the cubic phase which underwent heating at 22.1 GPa, according to the Birch–Murnaghan equation of state with $B'_0 = 4$ and a standard $V_0 = 158.43 \text{ \AA}^3$ ($a_0 = 5.411 \text{ \AA}$) of cubic CeO₂. This B_0 is less than former experimental values.

As shown above, the Raman spectra of the PbCl₂-type structure recorded in area 1 show complete phase transition; however, the x-ray diffraction pattern collected from area 1 shows mixed phases of cubic and orthorhombic structure. This is because the Raman spectra recorded the superficial information from the intensively heated side of the sample, and the x-ray diffraction collected the whole structural information of the sample in area 1.

4. Conclusions

This study has displayed the remarkable effects of high temperature on the behavior of CeO₂ at high pressures. Besides promoting a phase transition from the fluorite phase to a PbCl₂-type structure and reducing the phase transition pressure by nearly 20 GPa, high temperature also anneals the sample, which reaches its equilibrium state, and leads to about 1% decrease in volume at 22.1 GPa compared to the same fluorite phase at room temperature. The volume difference between the fluorite phase and PbCl₂-type phase is about 6.4% at a pressure of 22.1 GPa after heating, and the bulk modulus of the cubic structure of CeO₂ was calculated to be 200 GPa, assuming a pressure derivative of 4. The bulk modulus of the fluorite phase and the volume collapse induced by the phase transition of CeO₂ after heating are smaller than corresponding values obtained at room temperature by previous x-ray diffraction experiments. The effects of high temperature on CeO₂ should also be considered in the high-pressure behavior of other large metal-ion oxides, such as ThO₂, UO₂, and rare earth sesquioxides.

Acknowledgments

The authors are grateful for the support by Knowledge Innovation Program grant No. KJ CX2-SW-N20 sponsored by the Chinese Academy of Sciences and major research plan of NSFC-North China craton destruction, and partial support by BSRF. We also thank the Photon Factory for providing synchrotron beamtime under Proposal No. 2006G054.

References

- [1] Trovarelli A 1996 *Catal. Rev. Sci. Eng.* **38** 439
- [2] Walkenhorst A, Schmitt M, Adrian H and Petersen K 1994 *Appl. Phys. Lett.* **64** 1871
- [3] Weber W H, Hass K C and McBride J R 1993 *Phys. Rev. B* **48** 178
- [4] Hung V V, Lee J C and Masuda-Jindo K 2006 *J. Phys. Chem. Solids* **67** 682
- [5] Voloshina E and Paulus B 2006 *J. Chem. Phys.* **124** 234711
- [6] Hay P J, Martin R L, Uddin J and Scuseria G E 2006 *J. Chem. Phys.* **125** 034712
- [7] Kourouklis G A, Jayaraman A and Espinosa G P 1988 *Phys. Rev. B* **37** 4250
- [8] Duclos S J, Vohra Y K and Ruoff A L 1988 *Phys. Rev. B* **38** 7755
- [9] Gerward L and Olsen J S 1993 *Powder Diffr.* **8** 127
- [10] Rekihi S, Saxena S K and Lazor P 2001 *J. Appl. Phys.* **89** 2968
- [11] Wang Z W, Saxena S K, Pischedda V, Liermann H P and Zha C S 2001 *Phys. Rev. B* **64** 012102
- [12] Wang Z W, Zhao Y, Schiferl D, Zha C S and Downs R T 2004 *Appl. Phys. Lett.* **85** 124
- [13] Jayaraman A, Kourouklis G A and Uitert L G V 1988 *Pramana J. Phys.* **30** 225
- [14] Jayaraman A and Kourouklis G A 1991 *Pramana J. Phys.* **36** 133
- [15] Gerward L, Olsen J S, Petit L, Vaitheeswaran G, Kanchana V and Svane A 2005 *J. Alloys Compounds* **400** 56
- [16] Gerward L, Olsen J S, Steenstrup S, Malinowski M, Åsbrink S and Waskowska A 1992 *J. Appl. Crystallogr.* **25** 578
- [17] Francisco E, Blanco M A and Sanjurjo G 2001 *Phys. Rev. B* **63** 094107
- [18] Kanchana V, Vaitheeswaran G and Rajagopalan M 2003 *J. Alloys Compounds* **359** 66
- [19] Lazicki A, Yoo C S, Evans W J and Pickett W E 2006 *Phys. Rev. B* **73** 184120
- [20] Skorodumova N V, Ahuja R, Simak S I, Abrikosov I A, Johansson B and Lundqvist B I 2001 *Phys. Rev. B* **64** 115108
- [21] Mehrotra S, Sharma P, Rajagopalan M and Bandyopadhyay A K 2006 *Solid State Commun.* **140** 313
- [22] Kessler J R, Monberg E and Nicol M 1974 *J. Chem. Phys.* **60** 5057
- [23] Adachi G Y and Imanaka N 1998 *Chem. Rev.* **98** 1479
- [24] Liu L G 1980 *Earth Planet Sci. Lett.* **49** 166
- [25] Mao H K, Xu J and Bell P M 1986 *J. Geophys. Res.* **91** 4673
- [26] Keramidis V G and White W B 1973 *J. Chem. Phys.* **59** 1561
- [27] Takemura K 2001 *J. Appl. Phys.* **89** 662
- [28] Yang Z, Woo T K, Baudin M and Hermansson K 2004 *J. Chem. Phys.* **120** 7741
- [29] Hill S E and Catlow C R A 1993 *J. Phys. Chem. Solids* **54** 411